

PAPER • OPEN ACCESS

Positron-Positronium Converters in Reflection and Transmission Geometry for Gravitational Experiments with Antihydrogen using Moiré Deflectometry

To cite this article: R C Ferguson *et al* 2025 *J. Phys.: Conf. Ser.* **3029** 012005

View the [article online](#) for updates and enhancements.

You may also like

- [Application of Mullite Nanowhisker-reinforced Polyurethane Composites in 3D Printing](#)
Canyan Long, Xiaohua Gu, Wenkai Wen et al.
- [Offshore wakes measured by an adaptive dual-Doppler scanning lidar system](#)
Tabea Hildebrand, Florian Jäger, Nathalie Gloria et al.
- [Atomic Clock Ensemble in Space](#)
L. Cacciapuoti, A. Busso, R. Jansen et al.

Positron-Positronium Converters in Reflection and Transmission Geometry for Gravitational Experiments with Antihydrogen using Moiré Deflectometry

R C Ferguson^{1,2}, S Alfaro Campos^{3,4}, M Auzins⁵, M Berghold⁶, B Bergmann⁷, P Burian⁷, R S Brusa^{1,2}, A Camper⁸, R Caravita², F Castelli^{9,10}, G Cerchiari^{3,4}, R Ciuryło¹¹, A Chehaimi^{1,2}, G Consolati^{9,12}, M Doser¹³, K Eliaszuk¹⁴, M Germann¹³, A Giszczak¹⁴, L T Glögler¹³, Ł Graczykowski¹⁴, M Grosbart¹³, F Guatieri^{6,1,2}, N Gusakova^{13,15}, F Gustafsson¹³, S Haider¹³, S Huck^{13,16}, C Hugenschmidt⁶, M A Janik¹⁴, T Januszek¹⁴, G Kasprowicz¹⁷, K Kempny¹⁴, G Khatri¹³, Ł Kłosowski¹¹, G Kornakov¹⁴, V Krumins^{13,5}, L Lappo¹⁴, A Linek¹¹, S Mariazzi^{1,2}, P Moskal^{18,19}, M Münster⁶, P Pandey^{18,19}, D Pecak²⁰, L Penasa^{1,2}, V Petracek⁷, M Piwiński¹¹, S Pospisil⁷, L Povolo^{1,2}, F Prelz⁹, S A Rangwala²¹, T Rauschendorfer^{13,22}, B S Rawat^{23,24}, B Rienäcker²³, V Rodin²³, O M Røhne⁸, H Sandaker⁸, S Sharma^{18,19}, P Smolyanskiy⁷, T Sowiński²⁰, D Tefelski¹⁴, T Vafeiadis¹³, M Volponi¹³, C P Welsch^{23,24}, M Zawada¹¹, J Zielinski¹⁴, N Zurlo^{25,26}

1. Department of Physics, University of Trento, via Sommarive 14, 38123 Povo, Trento, Italy
2. TIFPA/INFN Trento, via Sommarive 14, 38123 Povo, Trento, Italy
3. University of Siegen, Department of Physics, Walter-Flex-Strasse 3, 57072 Siegen, Germany
4. Institut für Experimentalphysik, Universität Innsbruck, Technikerstrasse 25/4, 6020 Innsbruck, Austria
5. University of Latvia, Department of Physics Raina boulevard 19, LV-1586, Riga, Latvia
6. Heinz Maier Leibnitz Zentrum (MLZ), Technical University of Munich, Lichtenbergstraße 1, 85748, Garching, Germany
7. Institute of Experimental and Applied Physics, Czech Technical University in Prague, Husova 240/5, 110 00, Prague 1, Czech Republic
8. Department of Physics, University of Oslo, Sem Sælandsvei 24, 0371 Oslo, Norway
9. INFN Milano, via Celoria 16, 20133 Milano, Italy
10. Department of Physics “Aldo Pontremoli”, University of Milano, via Celoria 16, 20133 Milano, Italy
11. Institute of Physics, Faculty of Physics, Astronomy, and Informatics, Nicolaus Copernicus University in Toruń, Grudziadzka 5, 87-100 Toruń, Poland
12. Department of Aerospace Science and Technology, Politecnico di Milano, via La Masa 34, 20156 Milano, Italy
13. Physics Department, CERN, 1211 Geneva 23, Switzerland
14. Warsaw University of Technology, Faculty of Physics, ul. Koszykowa 75, 00-662, Warsaw, Poland
15. Department of Physics, NTNU, Norwegian University of Science and Technology, Trondheim, Norway
16. Institute for Experimental Physics, Universität Hamburg, 22607, Hamburg, Germany
17. Warsaw University of Technology, Faculty of Electronics and Information Technology, ul. Nowowiejska 15/19, 00-665 Warsaw, Poland
18. Marian Smoluchowski Institute of Physics, Jagiellonian University, Kraków, Poland
19. Centre for Theranostics, Jagiellonian University, Kraków, Poland



20. Institute of Physics, Polish Academy of Sciences, Aleja Lotnikow 32/46, PL-02668 Warsaw, Poland

21. Raman Research Institute, C. V. Raman Avenue, Sadashivanagar, Bangalore 560080, India

22. Felix Bloch Institute for Solid State Physics, Universität Leipzig, 04103 Leipzig, Germany

23. Department of Physics, University of Liverpool, Liverpool L69 3BX, UK

24. The Cockcroft Institute, Daresbury, Warrington WA4 4AD, UK

25. INFN Pavia, via Bassi 6, 27100 Pavia, Italy

26. Department of Civil, Environmental, Architectural Engineering and Mathematics, University of Brescia, via Branze 43, 25123 Brescia, Italy

E-mail: rileycraig.ferguson@unitn.it

Abstract. In the context of the Antihydrogen Experiment: Gravity, Interferometry, Spectroscopy (AEgIS) located at CERN, positron-positronium converters with a high positron-positronium conversion efficiency have been designed in both reflection and transmission geometries. The converters utilize nanochanneled silicon target technology with positron conversion efficiencies up to around 50% and around 16%, at room temperature and in the absence of magnetic fields, for reflection and transmission respectively. The positron-positronium converters allow for the pulsed production of antihydrogen ($\bar{\text{H}}$) within the AEgIS experiment. This paper discusses the use of a pulsed $\bar{\text{H}}$ beam in a moiré deflectometer to perform a precise gravitational measurement on $\bar{\text{H}}$ at AEgIS. This work describes the principles and technical details of the current design of a moiré deflectometer using the pulsed $\bar{\text{H}}$ beam. The main goal of this work is to summarize the ongoing project of adding the described moiré deflectometer to the AEgIS experiment to further their efforts toward probing the material dependence of gravity and testing the weak equivalence principle (WEP).

1 Introduction

A precision measurement of the acceleration due to gravity on antimatter provides a test on fundamental interactions and symmetries in nature, more specifically it is a test of the weak equivalence principle[1][2][3][4]. In the last few decades, several investigations[5][6][7] have chosen their antimatter system of interest to be antihydrogen ($\bar{\text{H}}$). A specified goal of the AEgIS collaboration is to directly detect gravitational acceleration using an $\bar{\text{H}}$ beam[8][9] combined with a moiré deflectometer[10], an instrument to perform high precision acceleration measurements.

The primary ingredients required for synthesizing $\bar{\text{H}}$ are positrons (e^+) and antiprotons (\bar{p}). The two most common methods for positron production are pair production and radioactive decay. ^{22}Na is the isotope used by AEgIS to produce positrons, and the capabilities of the AEgIS positron source will be discussed later in the Experimental section. To produce antiprotons, the Antimatter Factory utilizes pair production by colliding proton beams on an Ir target. Eq. 1 shows the reaction that produces antiprotons under the conservation requirements of energy, momentum, and nucleon number. The minimum kinetic energy of the incoming proton that is needed for this process is around 6 GeV and results in antiprotons on the scale of 1 GeV. The antiproton decelerator (AD) and Extra Low ENERGY Antiproton (ELENA) ring provide significantly slower antiprotons to AEgIS and other experiments of the Antimatter Factory[11].



The synthesis of $\bar{\text{H}}$ is generally achieved in experiment using 3 primary methods: radiative recombination[12][13], three-body recombination via "mixing"[14], and three-body recombination via charge exchange[15]. Radiative recombination and three-body recombination via "mixing" are not chosen within AEgIS due to the difficulty to scale and the difficulty to procure a time-signature, respectively. The method that is utilized in AEgIS is three-body recombination via charge exchange, shown in Eq. 2, which involves the laser-excited Rydberg states of both P_s and $\bar{\text{H}}$, denoted as P_s^* and $\bar{\text{H}}^*$ respectively. This method provides a clear time signature for the reaction with laser-excitation and is limited primarily by P_s availability.



Due to this method requiring excited Rydberg positronium (P_s^*), nanochanneled silicon positron-positronium converters have been developed in AEgIS. The converters have been shown to provide high conversion efficiencies, up to 50% in reflection converters[16][17] [18], at less than 1 keV positron implantation energies, and up to 16% for transmission converters, demonstrated with multiple membrane thicknesses that required different positron

implantation energies depending on sample[19]. Both transmission and reflection geometry converters were tested at room temperature and in the absence of magnetic fields. Within AEGIS, the converter is located on the axis of the antiproton magnetic trap. When a reflection converter is employed (see Fig. 1), a cone of Ps reflected back to the trap is produced. Ps is then laser-excited to Rydberg states ($n > 20$) [20][21][22]. The laser pulse provides a time signature for the formation of Rydberg \bar{H} . In the case of a transmission positron-positronium converter, the cone of Ps would be positioned upstream of the trapped antiprotons. Therefore, to achieve an \bar{H} beam the antiprotons need to be bunched from earlier in the apparatus in order to reach the Ps cloud in the back end of the trap. In order to obtain a beam of \bar{H} after a high magnetic field trap, to ultimately enter the moiré deflectometer, it is important to understand how atoms behave in a non-uniform magnetic field. Within AEGIS, Rydberg \bar{H}^* exits a 1 T solenoid magnet and experiences a non-uniform magnetic field and undergo the Zeeman effect, therefore \bar{H}^* either aligns or opposes the magnetic field, based on the spin of the positron[23]. This results in low magnetic field seeking and high magnetic field seeking \bar{H} , which would be on axis or on the fringes of the solenoid, respectively. Therefore, only low field seeking \bar{H} is retained to form a beam.

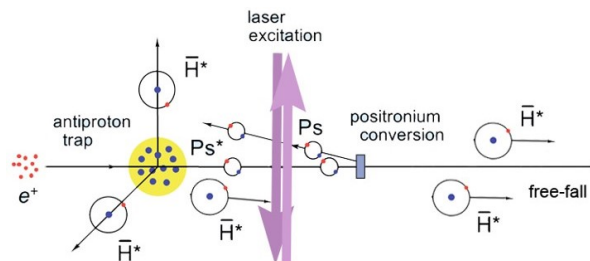


Figure 1: This schematic illustrates how \bar{H} is produced within the magnetic traps of AEGIS, when a positron-positronium converter is used. [20][21]

Moiré deflectometers are advanced optical devices used to measure the deflection of particles (such as antimatter) in the presence of external fields, particularly gravitational fields[10]. The underlying principle of these devices is based on the moiré effect[24], which occurs when two or more periodic patterns (often grids or gratings) are overlaid, creating interference fringes that can be used to detect tiny shifts or displacements. Fig. 2 illustrates the concept of moiré deflectometry that AEGIS will utilize for gravitational measurements[10][25]. Trajectories of both massive particles, under the effect of gravitation, and of undeflected particles. Massive particles experience a vertical shift in the final moiré pattern when compared to undeflected particles. The vertical shift, Δy can be calculated from acceleration, a , and time, τ using kinematics with $\Delta y = a\tau^2$, with $\tau = Lv_z^{-1}$, where L is the length between two successive gratings and v_z is the axial velocity. The vertical shift observed in the moiré are compared to the signal observed from horizontally aligned gratings, providing information on vertical and horizontal external forces in the environment. The minimum acceleration that can be observed is dependent on the period of the gratings, the interferometer visibility, time of flight, and the number of detected events[26].

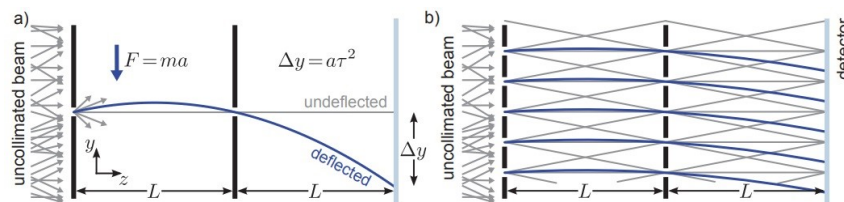


Figure 2: The difference in trajectories of a massive particle (blue) and an undeflected particle (gray) from a single slit grating are shown (a). Several trajectories from multiple slit grating are shown (b).[27]

For an apparatus length of 1 m and assuming a Maxwellian distribution of the particles peaked around a few Kelvins (corresponding to a mean velocity of 400 m s^{-1}), it leads to a typical spatial shift of $50 \mu\text{m}$ for a gravitational acceleration $a = 9.81 \text{ m s}^{-2}$ [25]. In the AEGIS design the moiré deflectometer is hosted in a 1 m ultra-high vacuum chamber. It can be rotated by 90 degrees, allowing measurements with the grating in vertical and horizontal position. A scintillator detector is used to monitor the beam lost on the grids while a novel system based on CMOS technology with micrometer resolution for event detection after the grids. In the following, we will detail the design and technical details of the moiré deflectometer to be implemented in AEGIS.

2 Experimental

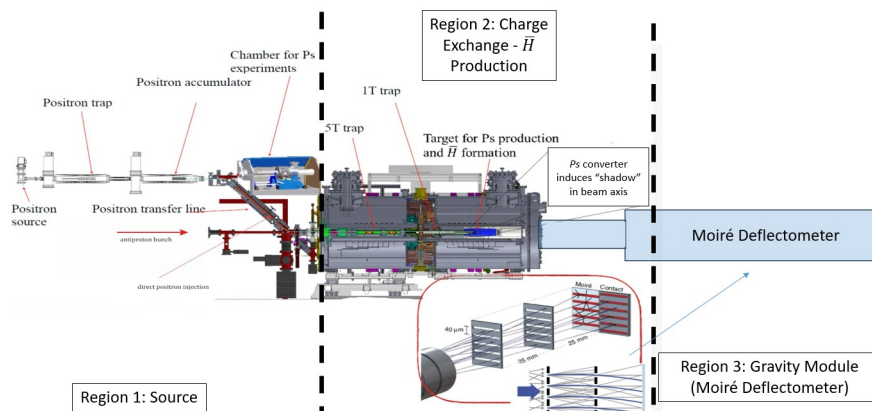


Figure 3: The AEGIS apparatus separated into source, \bar{H} production, and moiré deflectometer regions.

The AEGIS apparatus consists of three regions, as shown in Fig. 3, referred to as the source region, the \bar{H} production region, and the moiré deflectometer region. The source region consists of a ^{22}Na radioactive source for positrons, which can be redirected to a separate line and target chamber for positron and Ps research, and a beam line coming from the ELENA ring providing antiprotons for AEGIS. The positron source used in AEGIS is a ^{22}Na with a strength of 40 mCi and a moderator efficiency of 2.5×10^{-3} , as of November 2024. Positrons are cooled within a Surko trap outside a 5 T magnet, while antiprotons are stored and cooled within a Penning-Malmberg trap within the 5 T magnet apparatus. In the 1 T solenoid magnet, \bar{H} production occurs via the charge exchange process. This region contains the positron-positronium converter and the pulsed laser excitation of Ps , whose formation and excitation efficiency is monitored by means of micro-channel plate detector [28]. The converter induces a shadow on the produced \bar{H} flying towards the exit of the solenoidal magnet. Upon exiting the solenoid magnetic trap of the \bar{H} production region, the non-uniform field causes \bar{H} to undergo the Zeeman effect and some \bar{H} to be focused into the beam line. The recovery efficiency of \bar{H} back onto axis is currently being studied and simulated at AEGIS.

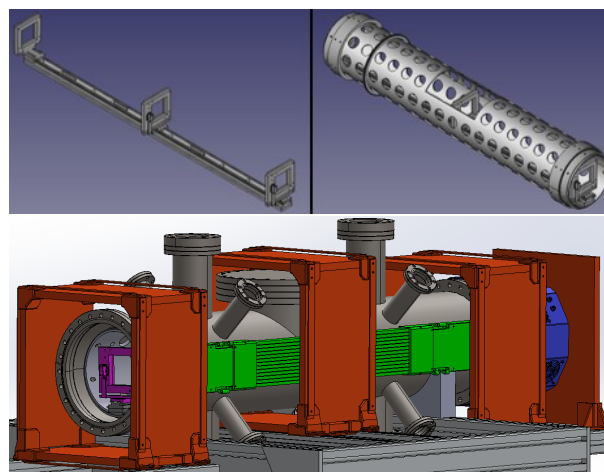


Figure 4: 3D drawing for the inner most section of the tube, the linear guide holding the moiré gratings (top left). The linear guide fixed to the rotating tube (top right). 3D drawing of the gravity module to be attached to AEGIS (bottom). Grating holders (pink), box scintillator detectors (red), JPET scintillator detector (green), and OPHANIM camera system (blue) is shown.

3 Development

The primary intent of this work is to discuss the development and status of the moiré deflectometer region, also referred to as the gravity module. The current design consists of a 1 m long linear apparatus fixed within a steel tube that can rotate either 90 degrees clockwise or counterclockwise. Two of the grating holders contain a Piezo motor that allows fine-tuning of the gratings to ensure proper alignment. The moiré gratings are made using electrochemical etching on Si wafers, where for our purposes the openings of the gratings will be 40 μm with 100 μm [29]. The inner linear guide and the rotating tube apparatus can be shown in Fig. 4. This moiré apparatus is secured to a CF 200 stainless steel pipe where scintillating detector boxes are placed around the locations of the moiré gratings to measure annihilation at each grating, as shown in Fig. 4. Furthermore, a JPET scintillator will be attached to one side of the assembly for full-length tracking of annihilation radiation over the entire gravity module [30]. In between the scintillator boxes, several flanges have been added to maximize access to the system. One radial CF 63 flange is for the gearbox to rotate the moiré deflectometer, two radial CF 63 flanges are for getter pumps, and two radial CF 150 flanges are for turbo pumps. The grating holders will contain environmental detecting sensors to measure temperature and magnetic field, and all relevant cables utilize the remaining radial CF ports.

Located at the end of the moiré apparatus will be a novel imaging system currently being designed by AEGIS, called the Optical Photon and Antimatter Imager (OPHANIM). This system is a vertexing detector based on a commercial mobile camera sensor. This detector is sensitive to e^+ , e^- , \bar{p} , kaons, pions, XUV light, and visible light.

4 Conclusions

This paper describes the installation of a gravity module, a moiré deflectometer, on the ongoing AEGIS experiment, a critical step required to directly detect gravitational acceleration using \bar{H} . The design is contingent on the creation of a low-energy pulsed Rydberg \bar{H} beam via the charge exchange reaction of antiprotons with Rydberg Ps , with Ps that is generated from an innovative nanochanneled silicon positron-positronium converter in reflection geometry. Some of the \bar{H} produced forms a beam that arrives to the moiré deflectometer, travels through the moiré gratings, and the arrival position of \bar{H} is measured on the OPHANIM detector. Losses inside the apparatus are monitored from scintillating detector boxes and event-vertexing JPET scintillators, all of which is secured to the external vacuum chamber previously described. The completion of this gravity module, expected within 2025, will be a monumental advancement in the direct observation of gravitational acceleration and provide an unprecedented low-energy pulsed beam of \bar{H} .

5 Acknowledgements

The AEGIS collaboration acknowledges the following funding agencies for their support. Istituto Nazionale di Fisica Nucleare; the CERN Fellowship programme and the CERN Doctoral student programme; the EPSRC of UK under grant number EP/X014851/1; Research Council of Norway under Grant Agreement No. 303337 and NorCC; CERN-NTNU doctoral program; the Research University – Excellence Initiative of Warsaw University of Technology via the strategic funds of the Priority Research Centre of High Energy Physics and Experimental Techniques; the IDUB POSTDOC programme; the Polish National Science Centre under agreements no. 2022/45/B/ST2/02029, and no. 2022/46/E/ST2/00255, and by the Polish Ministry of Education and Science under agreement no. 2022/WK/06; Marie Skłodowska-Curie Innovative Training Network Fellowship of the European Commission's Horizon 2020 Programme (No. 721559 AVA); European Union's Horizon 2020 research and innovation programme under the Marie Skłodowska-Curie grant agreement ANGRAM No. 748826; Wolfgang Gentner Programme of the German Federal Ministry of Education and Research (grant no. 13E18CHA); European Research Council under the European Unions Seventh Framework Program FP7/2007-2013 (Grants Nos. 291242 and 277762); the European Social Fund within the framework of realizing the project, in support of intersectoral mobility and quality enhancement of research teams at Czech Technical University in Prague (Grant No. CZ.1.07/2.3.00/30.0034). The AEGIS collaboration thanks the CERN accelerator and decelerator teams for the outstanding performance of the AD-ELENA complex.

References

- [1] G. Galilei. Elsevier, Leiden, 1638.
- [2] E.G. Adelberger et al. *Progress in Particle and Nuclear Physics*, **62**(1):102–134, 2009.
- [3] S. Fray et al. *Physical Review Letters*, **93**(24):240404, 2004.
- [4] K. Kuroda and N. Mio. *PRL*, **62**(17):1941, 1989.
- [5] M. Amoretti et al. (ATHENA Collaboration). *Nature*, **419**(6906):456–459, 2002. ATHENA Collaboration.
- [6] P. Adrich et al. *EPJ C*, **83**:1004, 2023.
- [7] E.K. Anderson et al. *Nature*, **621**:716–722, 2023.
- [8] G. Drobychev et al. (AEGIS Collaboration). Technical Report SPSC-P-334, CERN, 2007.
- [9] M. Doser et al. (AEGIS Collaboration). *Classical and Quantum Gravity*, **29**(18):184009, 2012.
- [10] M. K. Oberthaler et al. *Phys. Rev. A*, **54**:3165–3176, 1996.
- [11] S. Maury et al. *Hyperfine Interactions*, **229**:105–115, 2014.
- [12] G. I. Budker and A. N. Skrinskii. *Soviet Physics Uspekhi*, **21**:277, 1978.
- [13] H. Herr et al. *Physics at LEAR with Low-Energy Cooled Antiprotons*. volume 17, page 659, 1984.
- [14] G. Gabrielse et al. *Hyperfine Interactions*, **44**:287, 1988.
- [15] C. Amsler et al. (AEGIS Collaboration). *Commun. Phys.*, **4**(1):19, 2021.
- [16] S. Mariazzi et al. *Phys. Rev. B*, **81**:235418, 2010.
- [17] S. Mariazzi et al. *Phys. Rev. Lett.*, **104**:243401, 2010.
- [18] S. Mariazzi et al. (AEGIS Collaboration). *J. Phys. B: At. Mol. Opt. Phys.*, **54**(8):085004, 2021.
- [19] S. Mariazzi et al. *Phys. Rev. B*, **105**:115422, 2022.
- [20] R. S. Brusa et al. (AEGIS Collaboration). *Journal of Physics: Conference Series*, **791**(1):012014, 2017.
- [21] M. Doser et al. (AEGIS Collaboration). *Phil. Trans. R. Soc. A*, **376**(2116):20170274, 2018.
- [22] S. Aghion et al. (AEGIS Collaboration). *Phys. Rev. A*, **94**:012507, 2016.
- [23] N. Kuroda et al. *Nature Communications*, **5**:3089, 2014.
- [24] I. Amidror. *The Theory of the Moiré Phenomenon: Volume I: Periodic Layers*, volume 38. 2009.
- [25] P. Lansonneur. Phd thesis, Université de Lyon, 2017.
- [26] P. Bräunig. Phd thesis, Heidelberg University, 2015.
- [27] S. Aghion et al. (AEGIS Collaboration). *Nature Commun.*, **5**:4538, 2014.
- [28] C. Amsler et al. (AEGIS Collaboration). *Nucl. Instrum. Methods Phys. Res., B*, **457**:44–48, 2019.
- [29] K. Jefimovs et al. *Adv. in Pat. Mat. and Proc. XXXIV*. volume 10146, page 101460L, 2017.
- [30] S. Sharma et al. *Journal of Instrumentation*, **18**(02):C02027, 2023.